# Advanced Multi-Receiver Position-Information-Aided Vector Tracking for Robust GPS Time Transfer to PMUs

Yuting Ng and Grace Xingxin Gao
University of Illinois at Urbana-Champaign

## Biographies

**Yuting Ng** is a Master's student in the Aerospace Engineering Department at the University of Illinois at Urbana-Champaign. She received her Bachelor's degree, graduating with university honors, from the Electrical and Computer Engineering Department at the same university in 2014.

**Grace Xingxin Gao** is an assistant professor in the Aerospace Engineering Department at the University of Illinois at Urbana-Champaign. She obtained her PhD from Stanford University in 2008. She was a research associate at Stanford University from 2008 to 2012.

## Abstract

Phasor Measurement Units (PMUs) provide time-synchronized, accurate and precise measurements of instantaneous voltages and currents at many locations across the electrical power system. The current state-of-the-art time transfer architecture for PMUs uses GPS time synchronization. The dependence on GPS for time synchronization introduces new vulnerabilities to a power system utilizing PMUs. Thus, in our prior work, we proposed and verified with experimental data the concept of using multi-receiver position-information-aided vector tracking (MRPIAVT) to provide accurate, robust and reliable GPS time transfer for PMUs [1].

The MRPIAVT architecture is improved upon in this paper, leading to Advanced MRPIAVT. Improvements include modification of the state estimation equations such that the state vector contains only the clock bias and clock drift states. Updated clock dependent process noise covariance matrix used in the Extended Kalman Filter (EKF). Increased pre-detection coherent integration timing. Hardware timing synchronization, additional sub-sample software timing synchronization and an increased sampling rate. We demonstrate with further experiments, the enhanced performance of Advanced MRPIAVT with respect to timing accuracy, jamming, multipath and data-level spoofing.

## I. Introduction

Three-phase electric power is a common mode of power transfer [2]. In three-phase electric power, there is a need to synchronize the relative phases of the voltages and currents throughout the power grid. In the event that the phases become desynchronized, the network becomes unstable and a power failure may occur [3].

Currently, the state of the power grid is estimated and monitored using Supervisory Control and Data Acquisition (SCADA), a technology developed in the 1960s. SCADA produces low-rate, unsynchronized measurements. Thus, state estimation equations are nonlinear and computationally expensive. This leads to delayed and non-dynamic control responses. On the other hand, Phasor Measurement Units (PMUs), also known as Synchronized Phasors (synchrophasors), provide high-fidelity, high-rate, synchronized measurements. This leads to fast, accurate state estimations which offers opportunities for advanced, dynamic control responses and improved post disturbance analyses [3]–[7].

The current state-of-the-art time transfer architecture for PMUs uses GPS time synchronization [8]. The dependence on GPS for time synchronization introduces new vulnerabilities to a power system utilizing synchrophasors [9]. The low received signal-to-noise ratio (SNR) and unencrypted nature of the civil GPS signals opens risks for malicious parties to easily jam [12], [13] and broadcast falsified civil GPS signals [14]–[18] with the intentions of altering the timing solutions provided by the GPS receivers connected to the synchrophasors [8], [10], [11].

In our prior work, given that the GPS receivers used by PMUs are static, we proposed and verified with experimental data, the concept of using single-receiver position-information-aided vector tracking (SRPIAVT) to provide accurate, robust and reliable GPS time transfer for synchrophasors [22], [23]. To further limit the avenues of attack available to the malicious party, we proposed multi-receiver position-information-aided vector tracking (MRPIAVT), with multiple receivers spaced apart in a fixed configuration, and a common stable external clock [1], [19]. The MRPIAVT architecture is an extension of the multi-receiver vector tracking (MRVT) architecture with additional focus placed specifically on the clock bias and clock drift states [20], [21]. This was achieved through specifying additional constraints: known, static receiving antenna locations and common stable external clock. The MRPIAVT architecture improves the accuracy of time solutions, and also demonstrates robustness against noise, jamming, meaconing and spoofing attacks [1].

In this paper, we continue the development of MRPIAVT, with special focus on the following improvements. 1) Modifi-

The authors are with the Department of Aerospace Engineering, University of Illinois at Urbana-Champaign, Urbana, IL 61801, USA. E-mail: yng5@illinois.edu, gracegao@illinois.edu.

cation of state estimation equations such that the state vector contains only the clock bias and clock drift states. In addition, the process noise covariance matrix used in the Extended Kalman Filter (EKF) is specified based on the specification of the external clock. This presents a more accurate representation of the system. 2) Increased pre-detection coherent integration timing to reduce measurement noise. 3) Hardware timing synchronization, additional software sub-sample timing synchronization; increased sampling rate.

We propose the above improvements for better accuracy, reliability and robustness of the timing solutions as compared to the results presented in our prior work [1]. To evaluate the effectiveness of the improvements, we further conduct field experiments. We demonstrate the enhanced performance of the MRPIAVT with improvements as compared to the results shown in our prior work.

This paper is organized as follows: Section II briefly describes the background, theory and implementation of SRPIAVT, with clock bias and clock drift states, within each individual receiver. Section III describes the theory, implementation and initialization of MRPIAVT. Section IV describes the experiments that were conducted using static receivers installed on the roof of a building. Finally, Section V concludes the paper.

## II. Single-Receiver Position-Information-Aided Vector Tracking (SRPIAVT)

Vector tracking was first proposed in 1996 as the Vector Delay Lock Loop (VDLL) by Spilker [24]. Similar to MRVT [20], [21], in MRPIAVT, within each individual receiver, we implement a variation of the non-coherent Vector Delay and Frequency Lock Loop (VD/FLL) using an Extended Kalman Filter (EKF) with a two step update process: measurement update and time update [25], [26]. For more details of the SRVT variation implemented, please refer to [21].

In SRPIAVT, the receiver's position and velocity are known quantities. Thus, the state vector in SRPIAVT only contains the clock bias and clock drift variables and is given as (1):

$$\begin{aligned} X \;&:\; \text{state vector} \\ &= \begin{bmatrix} c\delta t_u \\ c\dot{\delta t}_u \end{bmatrix} \\ c \;&:\; \text{speed of light, } 299792458, (ms^{-1}) \\ c\delta t_u \;&:\; \text{clock bias } (m) \\ c\dot{\delta t}_u \;&:\; \text{clock drift } (ms^{-1}) \end{aligned} \tag{1}$$

Along the same lines of reducing the receiver state vector to only the clock bias and clock drift variables, the modified geometry matrix $H$ in the EKF measurement update at time $k$ is given in (2).

$$\begin{aligned} H \;&:\; \text{geometry matrix} \\ &= \begin{bmatrix} 1 & \dots & 1 & & & \\ & & & 1 & \dots & 1 \end{bmatrix}^{\top} \\ 1 \;&:\; \text{scalar value 1} \end{aligned} \tag{2}$$

Similarly, for the EKF time update at time $k+1$, the state propagation matrix $F$ and state process noise covariance matrix $Q$ are modified. (3,4):

$$\begin{aligned} F \;&:\; \text{state propagation matrix} \\ &= \begin{bmatrix} 1 & \Delta T \\ 0 & 1 \end{bmatrix} \end{aligned} \tag{3}$$

$$\begin{aligned} Q \;&:\; \text{state process noise covariance matrix} \\ &= F \begin{bmatrix} (c \times \sigma_{\delta t})^2 & 0 \\ 0 & (c \times \sigma_{\delta \dot{t}})^2 \end{bmatrix} F^T \\ \sigma_{\delta t} \;&:\; \text{measure of oscillator phase deviation for } \Delta T \\ \sigma_{\delta \dot{t}} \;&:\; \text{measure of oscillator frequency deviation for } \Delta T \end{aligned} \tag{4}$$

The state process noise covariance matrix, $Q$ is set based on the specification of the external clock [28], [29] for $\Delta T$ measurement intervals. It is recommended that these parameters be measured using specialized equipment or consult the manufacturer. For the results published in this paper, $\sigma_{\delta \dot{t}}$ was set as $2.5e^{-10}$.

Finally, since the receivers in SRPIAVT are static, the coherent integration period can be longer. As a preliminary trial, the coherent integration period and measurement update interval, $\Delta T$, are the same and set to $\Delta T = 0.020s$.

## III. Multi-Receiver Position-Information-Aided Vector Tracking (MRPIAVT)

Similar to MRVT, in MRPIAVT, the corrected state vector $X$ of each receiver is used to determine the reference state vector $X_{ref}$. As the individual receivers are triggered by the same external clock, their clock drifts $c\dot{\delta t}_u$ are the same and their clock biases $c\delta t_u$ differ by a constant. These constraints are used to augment the VTL of the individual receivers. Fig.1 shows the overall information flow between the different entities involved: Channel, Receiver, Receiver Network.

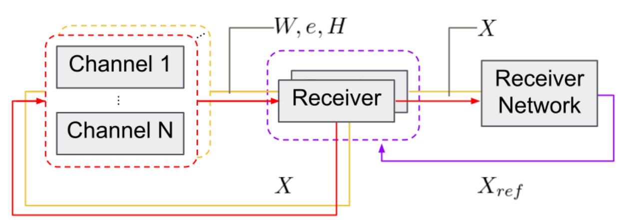


Fig. 1. MRVT architecture implemented in this paper.

### A. MRPIAVT Initialization

As MRPIAVT relies on position-information-aiding, the positions of the individual receivers is of utmost importance. In order to obtain more accurate positions and relative positions that conform to measured, known baseline constraints, Advanced MRVT [21] is used to determine the positions of the static receivers. After the MRVT solutions converge, these static positions are then used in MRPIAVT.

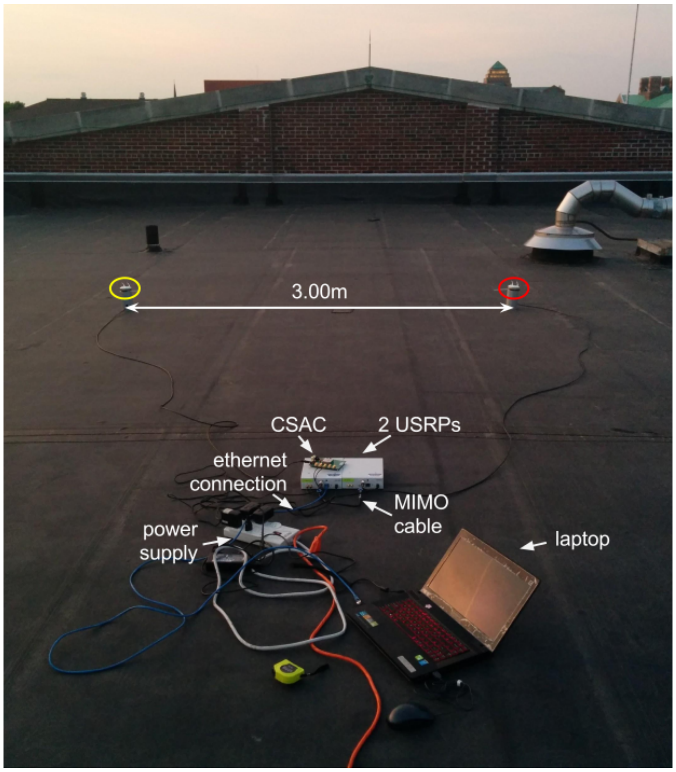


Fig. 2. Geometry of receiving antennas on the roof of Talbot Laboratory at the University of Illinois, at Urbana-Champaign. The two antennas are given a distinguishing color label, referenced in the figures of the results.

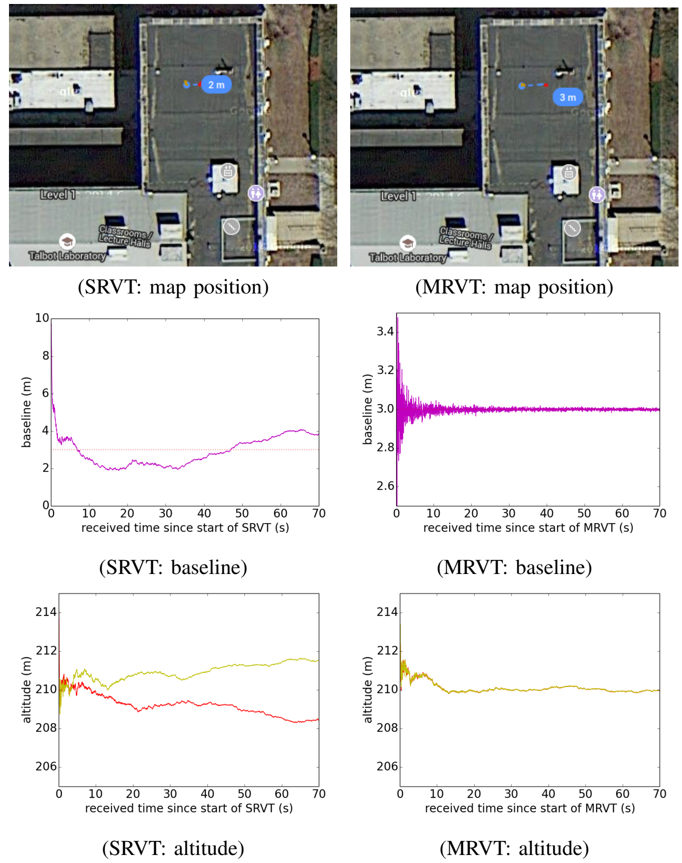


Fig. 3. Comparison of position-information obtained from SRVT and MRVT as displayed on Google - My Maps and as baselines distances and altitudes.

### *B. MRPIAVT Implementation*

Within the navigation filter of the Receiver Network, the reference clock bias is first determined. The state vector of each Receiver is then propagated in time to match the reference clock bias, providing sub-sample timing synchronization of the Receivers. The reference clock drift is then determined. This can be done through various methods, such as simple averaging or Kalman filtering. For the results shown in the next section, a simple averaging was performed. The updated reference state vector is then fed back to each individual Receiver, aiding their VTL. The EKF time update step then follows in each Receiver. In this manner, as compared to SRPIAVT [22], the state vectors of the individual receivers are further constrained base on the knowledge of the common external clock and the fixed receiver baselines. The reduction in the overall search space, offers increased robustness to noise, jamming and also provides more salient detection features for meaconing or spoofing attacks.

## IV. Experiments and Results

Experiments on the roof of a building were conducted to evaluate the performance of the MRPIAVT architecture.

Two AntCom 3GNSSA4-XT-1 GNSS antennas [30] were placed in a static configuration, 3 meters apart on the roof a building, as shown in Fig.2. Each antenna was connected to an Ettus Research USRP N210, equipped with a DBSRX2 daughterboard [31], [32]. The Universal Software Radio Peripherals (USRPs) were triggered by the same Microsemi Quantum SA.45s Chip Scale Atomic Clock (CSAC) [33]. To enable sample-level timing synchronization between the two USRPs, a MIMO cable was used to provide timing synchronization between the two USRPs. The complex GPS L1 raw signals were modulated to 0-IF, digitized at a sampling frequency of 5MHz and output as interleaved complex shorts. The output data were sent via ethernet and written directly onto the internal hard disk of a laptop running Ubuntu 14.04.

### *A. Position-Information-Aiding*

We evaluated the performance of MRVT against SRVT for use in determining the static receiver positions as is shown in Fig.3. Fig.3 shows the positions plotted on My Maps, a tool for generating custom maps developed by Google [34]; the estimated baseline distances, with the accurate baseline distance of 3m shown in red and the estimated altitudes. The residual in the up direction, or altitude, most directly affects the clock bias estimate.

Since MRVT produces position estimates with the least noise, most accurate baselines and altitudes, MRVT was the algorithm of choice for producing position-information-aiding for MRPIAVT.

### *B. Timing Results*

A comparison of the clock bias and clock drift results from SRVT and MRPIAVT is shown in Fig.4.

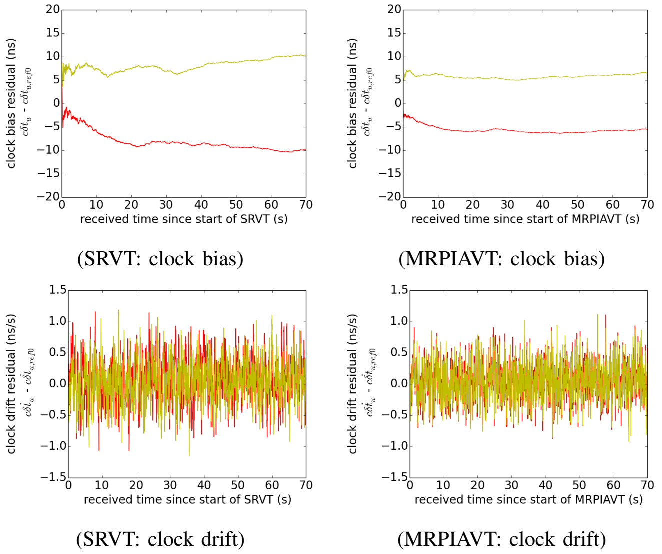


Fig. 4. Comparison of clock bias and clock solutions obtained from SRVT and MRPIAVT. The clock bias obtained from the individual receivers is different by a constant due to slight difference in propagation delay between signal reception at the antenna and baseband processing. Yellow and red lines belong to the two receivers shown in Fig.2.

From Fig.4, MRPIAVT exhibits less noise in the clock bias and clock drift solutions. In addition, the difference in clock bias between the individual receivers is maintained as a relative constant.

### C. Timing Attacks: Jamming

To test the robustness of MRPIAVT against jamming attacks, jamming signals of various noise levels were generated using GNURadio, as shown in Fig.5. As the noise level is increased, fewer satellites were successfully detected during acquisition, see TABLE I. In order to have a fair comparison, for all noise levels, a hot start assuming successful acquisition of 6 out of 6 satellites was applied.

TABLE I
NUMBER OF SATELLITES ACQUIRED UNDER VARIOUS SNR DEGRADATION

| SNR degradation (dB) | No. satellites acquired (out of 6) |
|---|---|
| -4.63 | 6 |
| -7.27 | 2 |
| -9.24 | 0 |
| -11.55 | 0 |
| -13.62 | 0 |
| -15.04 | 0 |

The clock bias and clock drift solutions of MRPIAVT is shown in Fig.6. From Fig.6, MRPIAVT is robust to jamming of at least -15dB.

### D. Timing Attacks: Meaconing

To evaluate the performance of MRPIAVT under meaconing attacks, two meaconing signals (weak and strong) were generated using GNURadio, as shown in Fig.7. The weak meaconing signal has the false and original signal at the same power level. The strong meaconing signal has the false signal at 20dB above the power level of the original signal. The meaconing attack took place 50s after the initialization of MRPIAVT.

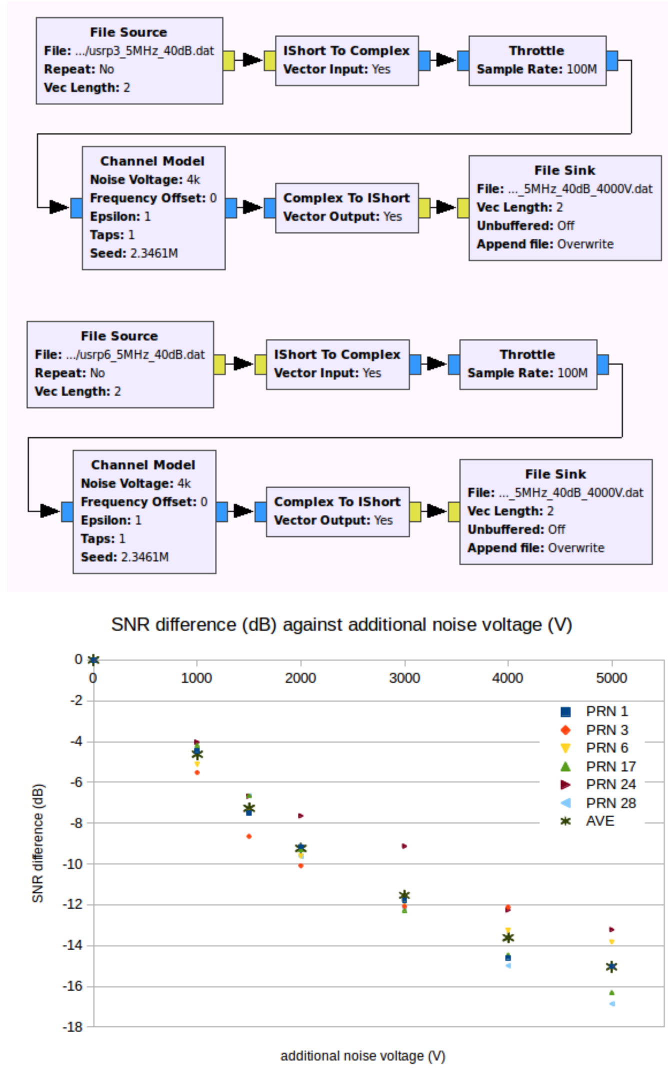


Fig. 5. GNURadio flow graph for generating the jamming signals and Graph of SNR difference (dB) against added noise voltage (V). In the GNURadio flow graph, the **IShort to Complex** block converts data samples saved in interleaved short format to a complex number. The **Throttle** block controls the post-processing computing speed. The **Channel Model** block generates and adds White Gaussian Noise (WGN) to the signal. The **Complex To IShort** block converts data samples represented as complex numbers back to interleaved shorts. For the graph of SNR difference (dB) against added noise voltage (V), noisy signals with approximately -4.63dB, -7.27dB, -9.24dB, -11.55dB, -13.62dB and -15.04dB difference in SNR were generated.

In the event of a weak meaconing attack, MRPIAVT remains robust and continues tracking the original clock bias and clock drift. In the event of a strong meaconing attack, MRPIAVT detects the attack.

### E. Timing Attacks: Data-level Spoofing

As a preliminary evaluation of the performance of MRPIAVT under spoofing attacks, a data-level spoofing attack

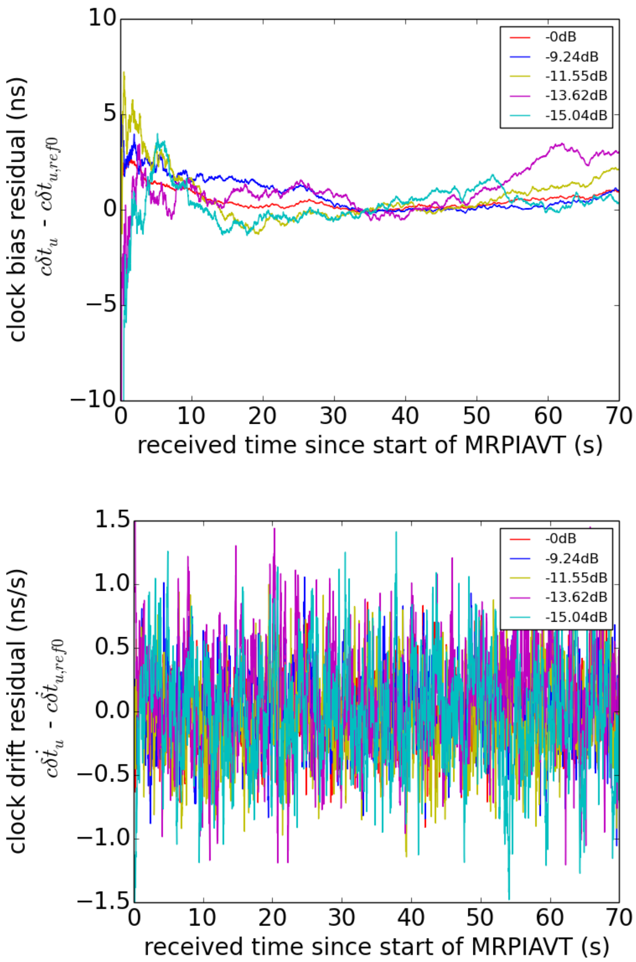


Fig. 6. Demonstrating robustness of MRPIAVT clock bias and clock drift solution to jamming. Shown are clock bias solutions from jamming conditions with SNR difference of 0dB to -15dB. The clock bias solutions from the noisy signals converge to the clock bias solution obtained from the signal with no additional noise jamming.

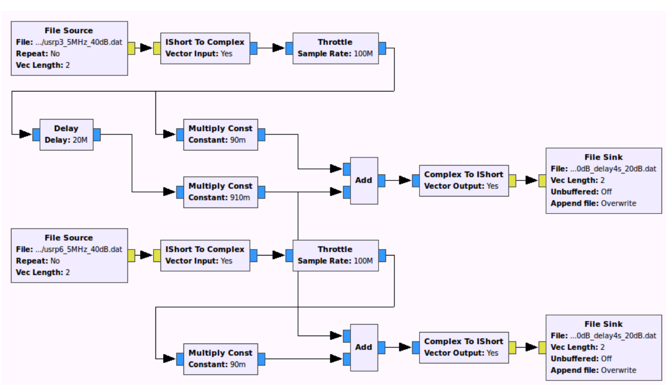


Fig. 7. GNURadio flow graph for generating the meaconing signals. The meaconing signal is overlayed on the original signal. The **IShort to Complex** block converts data samples saved in interleaved short format to a complex number. The **Throttle** block controls the post-processing computing speed. The **Delay** block delays the signal by a specified number of samples. The **Multiply Const** block multiplies the signal by a constant gain. The **Add** block sums the two signals. The **Complex To IShort** block converts data samples represented as complex numbers back to interleaved shorts.

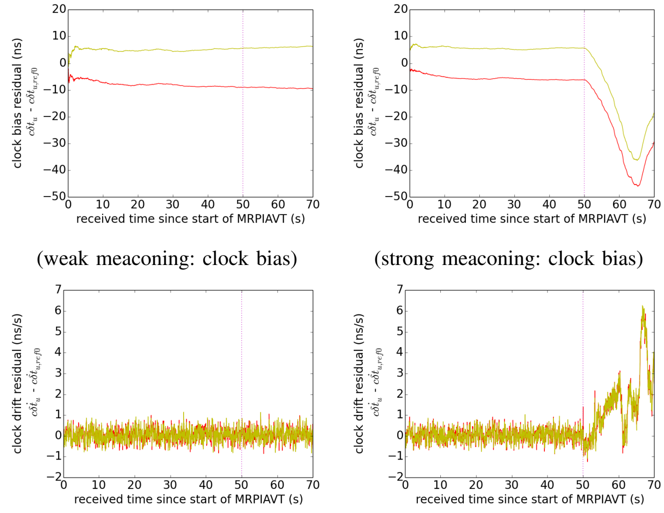


(weak meaconing: clock bias) (strong meaconing: clock bias)

(weak meaconing: clock drift) (strong meaconing: clock drift)

Fig. 8. Weak and strong meaconing attack at 50s. False and original signal at the same power level for the weak scenario. False signal at a power level of 20dB above the original signal for the strong scenario.

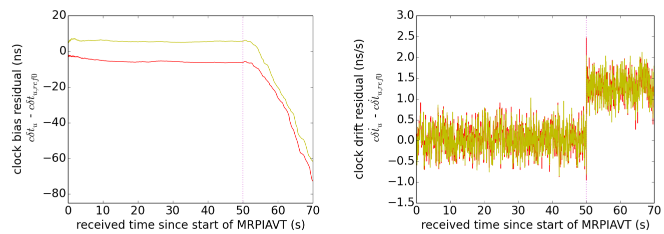


(data-level spoofing: clock bias) (data-level spoofing: clock drift)

Fig. 9. Data-level spoofing attack at 2000x20ms. All satellite clock biases were shifted by 4s.

was conducted in which the clock bias parameter in the ephemerides for all the satellites were shifted by 4s.

From Fig.9, similar to a strong meaconing attack, MRPIAVT detects the attack.

### *Summary of Experimental Results*

We have demonstrated the ability of MRPIAVT to provide more accurate, robust and reliable timing solutions as compared to SRVT.

The experimental results focusing on the timing attacks demonstrated the robustness of MRPIAVT to jamming and weak meaconing; MRPIAVT was also shown to successfully detect strong meaconing attacks and data-level spoofing.

## V. Conclusion

In conclusion, we have proposed the MRPIAVT architecture as an extension of SRPIAVT and MRVT. By reducing the search space from each individual Receiver to the Receiver Network, to just the timing variables of the Receiver Network, we have increased information redundancy which offers more accurate, reliable and robust timing solutions, especially under malicious attacks. We validated the performance of our proposed MRPIAVT architecture with experimental results.

## ACKNOWLEDGMENT

This work was supported in part by the Trustworthy Cyber Infrastructure for the Power Grid (TCIPG) under US Department of Energy Award DE-OE0000097.

The views and opinions of authors expressed herein do not necessarily state or reflect those of the United States Government or any agency thereof.

In addition, the authors would like to acknowledge Daniel Chou for his contributions, thank Ganshun Lim for encouragement and also thank Mr. Phil Ward for guidance and advice.

## REFERENCES

[1] D. Chou, Y. Ng, and G.X. Gao, "Robust GPS-Based Timing for PMUs Based on Multi-Receiver Position-Information-Aided Vector Tracking," *Proceedings of the 2015 International Technical Meeting of The Institute of Navigation*, Dana Point, California, January 2015.

[2] P.W. Sauer and M.A. Pai, *Power System Dynamics and Stability*, 7th ed. Stipes Publishing Co. 2007

[3] D.G. Hart, D. Uy, V. Gharpure, D. Novosel, D. Karlsson, M. Kaba, "PMUs A new approach topower network monitoring", *ABB Review*, 2001. Retrieved June 14, 2015 from https://library.e.abb.com/public/2d4253f3c1bff3c0c12572430075caa7/EDITORIAL_2001_04_en_PMUs_-_A_New_Approach_to_Power_Network_Monitoring.pdf

[4] U.S. Energy Information Administration, "New technology can improve electric power system efficiency and reliability," *Today in Energy*, Retrieved June 14, 2015 from http://www.eia.gov/todayinenergy/detail.cfm?id=5630

[5] Schweitzer Engineering Laboratories, "Making Sense of Synchrophasor Data," *The Synchrophasor Report*, Nov 2011, vol. 3, no. 5. Retrieved June 14, 2015 from https://www.selinc.com/TheSynchrophasorReport.aspx?id=98504

[6] Schweitzer Engineering Laboratories, "Improve Data Analysis by Time-Stamping Your Data," *The Synchrophasor Report*, May 2009, vol. 1, no. 3. Retrieved June 14, 2015 from https://www.selinc.com/issue3/

[7] Schweitzer Engineering Laboratories, "Use Time-Synchronized Phasors for Real-Time Control," *The Synchrophasor Report*, Aug 2009, vol. 1, no. 4. Retrieved June 14, 2015 from https://www.selinc.com/issue4/

[8] Schweitzer Engineering Laboratories, "Mitigating GPS Vulnerabilities," *The Synchrophasor Report*, Nov 2014, vol. 6, no. 4. Retrieved June 14, 2015 from https://www.selinc.com/TheSynchrophasorReport.aspx?id=106437

[9] L. Heng, J. Makela, A. Dominguez-Garcia, R. Bobba, W. Sanders, and G.X. Gao, "Reliable GPS-based Timing for Power System Applications: A multi-Layered Multi-receiver Approach," *Proceedings of the 2014 IEEE Power and Energy Conference at Illinois (IEEE PECI 2014)*, Champaign, IL, Feb 2014.

[10] X. Jiang, J. Zhang, B.J. Harding, J.J. Makela, and A.D. Dominguez-Garcia, "Spoofing GPS Receiver Clock Offset of Phasor Measurement Units," *IEEE Transactions on Power Systems*, vol. 28, no. 3, pp. 3253-3262, 2013.

[11] D.P. Shepard, T.E. Humphreys, and A.A. Fansler, "Evaluation of the vulnerability of phasor measurement units to GPS spoofing attacks," *International Journal of Critical Infrastructure Protection*, vol. 5, no. 3-4, December 2012, pp. 146-153

[12] C. Matyszczyk, "Truck driver has GPS jammer, accidentally jams Newark airport," *CNET Tech Culture*, Aug 11, 2013. Retrieved June 14, 2015 from http://www.cnet.com/news/truck-driver-has-gps-jammer-accidentally-jams-newark-airport/

[13] GPS World Staff, "Massive GPS Jamming Attack by North Korea," *GPS World*, May 8, 2012. Retrieved June 14, 2015 from http://gpsworld.com/massive-gps-jamming-attack-by-north-korea/

[14] T. Nighswander, B. Ledvina, J. Diamond, R. Brumley, D. Brumley, "GPS Software Attacks,", *Proceedings of the 2012 ACM Conference on Computer and Communications Security (CCS '12)*, Raleigh, North Carolina, USA, pp. 450-461. Retrieved June 14, 2015 from https://www.andrew.cmu.edu/user/tnighswa/GPS_CCS.pdf

[15] K. Wesson, D. Shepard, and T. Humphreys, "Straight Talk on Anti-SpoofingSecuring the Future of PNT," *GPS World*, January 2012. Retrieved June 14, 2015 from http://radionavlab.ae.utexas.edu/images/stories/files/papers/antiSpoofStraightTalk_Wesson.pdf

[16] S. Lo, D. D.Lorenzo, P. Enge, D. Akos, P. Bradley, "A Secure Civil GNSS for Today," *InsideGNSS: Signal Authentication*, Sep/Oct 2009. Retrieved June 14, 2015 from http://www.insidegnss.com/node/1633

[17] T.E. Humphreys, B.M. Ledvina, M.L. Psiaki, B.O. Hanlon, and P.M. Kintner, "Assessing the SpoofingThreat: Development of a Portable GPS Civilian Spoofer," *Proceedings of the Institute of Navigation GNSS (ION GNSS2008)*, 2008.

[18] L. Heng, D.B. Work, and G.X. Gao, "Reliability from Unreliable Peers: Cooperative GNSS Authentication," *Inside GNSS Magazine*, SeptemberOctober 2013.

[19] N.O. Tippenhauer, C. Pöpper, K.B. Rasmussen, and S. Capkun, "On the Requirements for Successful GPS Spoofing Attacks," *Proceedings of the 18th ACM Conference on Computer and Communications Security (CCS '11)*, Chicago, Illinois, USA, 2011, pp. 75-86. Retrieved June 14, 2015 from https://www.cs.ox.ac.uk/files/6489/gps.pdf

[20] Y. Ng, and G.X. Gao, "Multi-Receiver Vector Tracking Based on a Python Platform," *Proceedings of the 2015 International Technical Meeting of The Institute of Navigation*, Dana Point, California, January 2015, pp. 633-639.

[21] Y. Ng, and G.X. Gao, "Advanced Multi-Receiver Vector Tracking for Positioning a Land Vehicle," *Proceedings of the 26th International Technical Meeting of the Satellite Division of the Institute of Navigation (ION GNSS+ 2014)*, Tampa, Florida, September 2015.

[22] D. Chou, L. Heng, and G.X. Gao, "Robust GPS-Based Timing for Phasor Measurement Units: A Position-Information-Aided Approach," *Proceedings of the 27th International Technical Meeting of The Satellite Division of the Institute of Navigation (ION GNSS+ 2014)*, 2014.

[23] L. Heng, D. Chou, and G.X.Gao, "Reliable GPS-Based Timing for Power Systems: A Multi-Layered, Multi-Receiver Architecture," *Inside GNSS Magazine*, November-December 2014.

[24] Spilker Jr, J., "Vector Delay Locked Loop" in *Global Positioning System: Theory and Applications*, B. Parkinson, J. Spilker, P. Axelrad, and P. Enge, Eds. Washington, DC: American Institute of Aeronautics and Astronautics, 1996, vol. I, pp. 291-327

[25] S. Zhao, D. Akos, "An Open Source GPS/GNSS Vector Tracking Loop - Implementation, Filter Tuning, and Results," *Proceedings of the 2011 International Technical Meeting of The Institute of Navigation*, San Diego, CA, January 2011, pp. 1293-1305.

[26] S. Bhattacharyya, *Performance and Integrity Analysis of the Vector Tracking Architecture of GNSS Receivers*. PhD Dissertation, 39-114, 2012. Retrieved August 1, 2014, from http://www.aem.umn.edu/info/spotlight/bhattacharyya_thesis_final.pdf

[27] E. Kaplan, C. Hegarty, P. Ward, and J. Betz, "Chapter 5: Satellite Signal Acquisition, Tracking, and Data Demodulation," *Understanding GPS: Principles and applications* 2nd ed., pp. 153-240, Boston: Artech House, 2006.

[28] Microsemi, "QUANTUM Chip Scale Atomic Clock Product Info," Retrieved June 3, 2015, from http://www.microsemi.com/products/timing-synchronization-systems/csac#product-info

[29] F.D. Busse, J.P. How, J. Simpson, "Demonstration of Adaptive Extended Kalman Filter for Low-Earth-Orbit Formation Estimation Using CDGPS," *Navigation*, vol. 50, no. 2, Blackwell Publishing Ltd, 2161-4296, pp. 79-93, 2003.

[30] Antcom, "P/N: 3GNSSA4-XT-1," Retrieved June 20, 2015 from http://www.antcom.com/documents/catalogs/Page/3GNSSA4-XT-1_GNSSAntennas1.pdf

[31] Ettus Research, "USRP N210," Retrieved June 20, 2015 from http://www.ettus.com/product/details/UN210-KIT

[32] Ettus Research, "DBSRX2 800-2300 MHz Rx," Retrieved June 20, 2015 from http://www.ettus.com/product/details/DBSRX2

[33] Microsemi, "QUANTUM Chip Scale Atomic Clock," Retrieved June 20, 2015 from http://www.microsemi.com/products/timing-synchronization-systems/csac#overview

[34] Google, "My Maps," Retrieved June 3, 2015 from https://www.google.com/mymaps